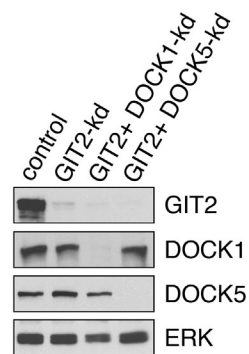


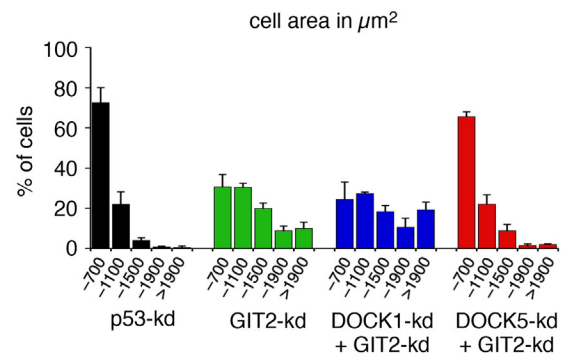
Supplementary Information

Supplementary Figure S1

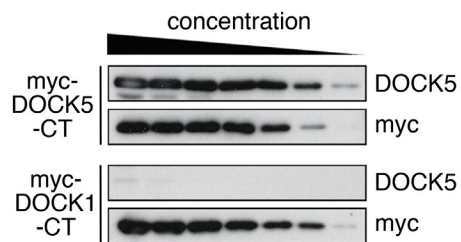
a



b



c



d

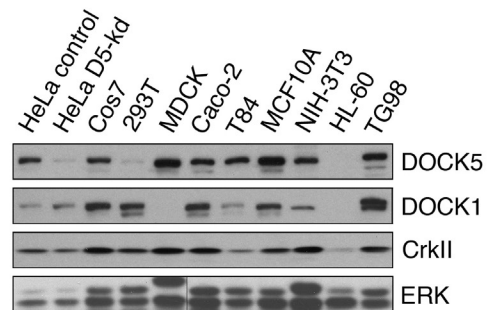
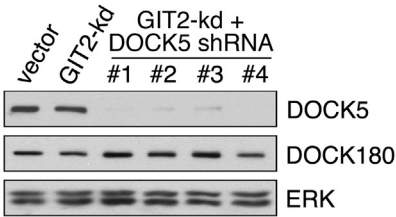


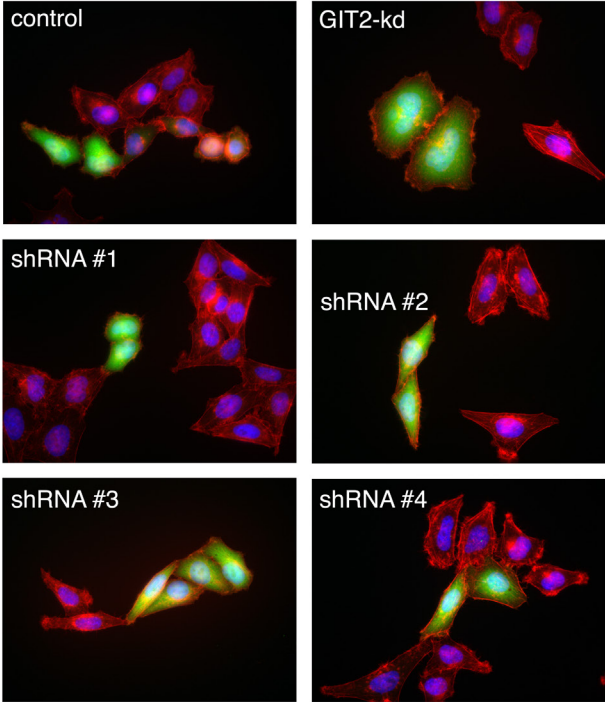
Figure S1. DOCK5, but not DOCK1, is repressed by GIT2. **(a)** Expression of GIT2, DOCK5, DOCK1, and ERK in pooled populations of HeLa cells with or without shRNA-mediated depletion of GIT2 alone or with siRNA-mediated co-depletion of DOCK1 or DOCK5. **(b)** Quantification of cell spreading assays showing the distribution of areas occupied by cells 1 h after plating on collagen. The data represent means \pm SD (n=3). **(c)** HeLa cells were transiently transfected with either Myc-tagged DOCK5-CT (top panels) or Myc-tagged DOCK1-CT (lower panels). Total cell lysates were subjected to 2-fold serial dilutions and blotted with DOCK5-specific antibodies. Equivalent samples were also blotted with Myc antibodies to allow for direct comparison of protein amounts. **(d)** Expression of DOCK5, DOCK1, CrkII, and ERK in a panel of mammalian cell lines. Specificity of DOCK5 antibody is evidenced by absence of reactivity in HeLa cells from which DOCK5 has been depleted by shRNA-mediated knockdown.

Supplementary Figure S2

a



b



c

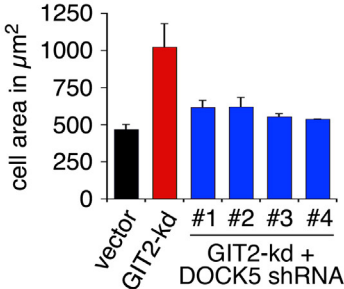


Figure S2. Repression of cell spreading in GIT2-depleted cells by knockdown of DOCK5 is not due to off-target effects. **(a)** Pooled HeLa cell lines were generated by retroviral transduction of shRNA expression vectors encoding four distinct DOCK5 targeting sequences. Cell lines were subsequently transfected with a GIT2 silencing vector expressing EGFP from a distinct cassette and processed for experimentation 48 h after plating. The shRNAs all yielded efficient knockdown of DOCK5 without affecting cellular levels of DOCK1 or ERK. **(b)** Depletion of GIT2 in HeLa cells induced cell spreading that was abrogated by each of the aforementioned four shRNAs for DOCK5. GIT2 shRNA targeted cells were identified by EGFP expression. Nuclei and actin are labeled with DRAQ5 and Alexa⁵⁹⁴-conjugated phalloidin, respectively. **(c)** Quantitative analysis of the effect of DOCK5 depletion on the cell area of GIT2-depleted cells. Data are represented as mean cell area +/- SD (n=3).

Supplementary Figure S3

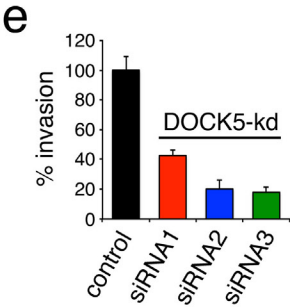
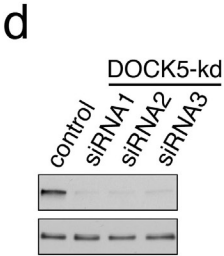
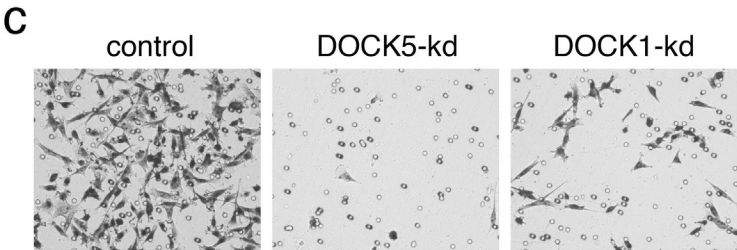
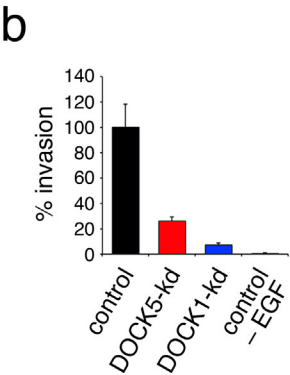
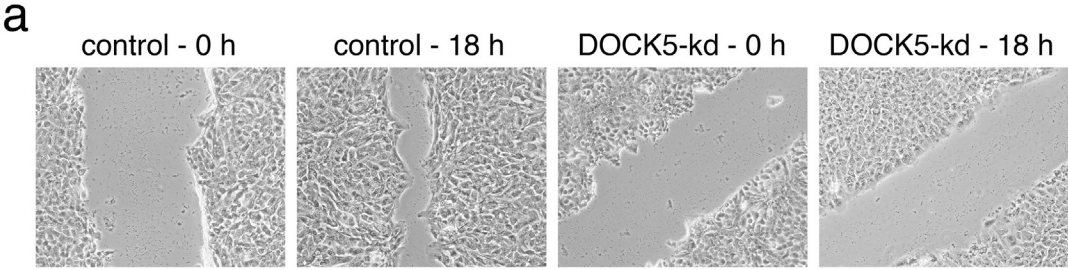
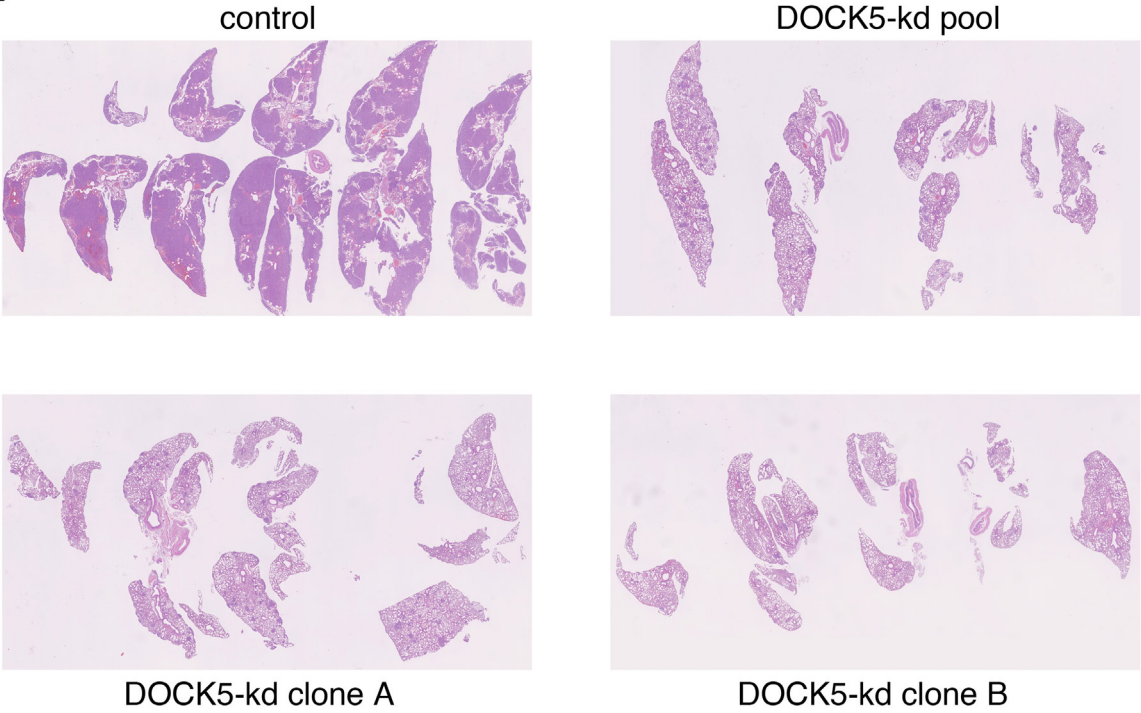


Figure S3. DOCK5 is required for epithelial migration and invasion. **(a)** MCF10A control cells or a pooled cell population stably expressing DOCK5 shRNA were cultured on fibronectin-coated coverslips and “scratch wounded” with a p200 pipette tip. Wounds were imaged by phase contrast microscopy at 0 h and 18 h. **(b)** To quantify changes in MDA-MB-231 invasion, control (black), DOCK5-kd (red), or DOCK1-kd (blue) cells were harvested and added to the top chamber of Matrigel-coated transwell filters and incubated for 12 h with or without 10 ng/ml of EGF as a chemoattractant. Cells that migrated to the bottom chamber were quantified. Values are means \pm SD (n=3). **(c)** Representative trypan blue staining of MDA-MB-231 control, DOCK5-kd, and DOCK1-kd cells having migrated to the bottom of Matrigel-coated transwell filter when 10% serum is used as a chemoattractant. **(d)** Depletion of DOCK5 from MDA-MB-231 cells using three additional siRNAs targeting DOCK5 message. **(e)** Invasion assays performed with cells described in (d). Values are means \pm SD (n=3).

Supplementary Figure S4

a



b

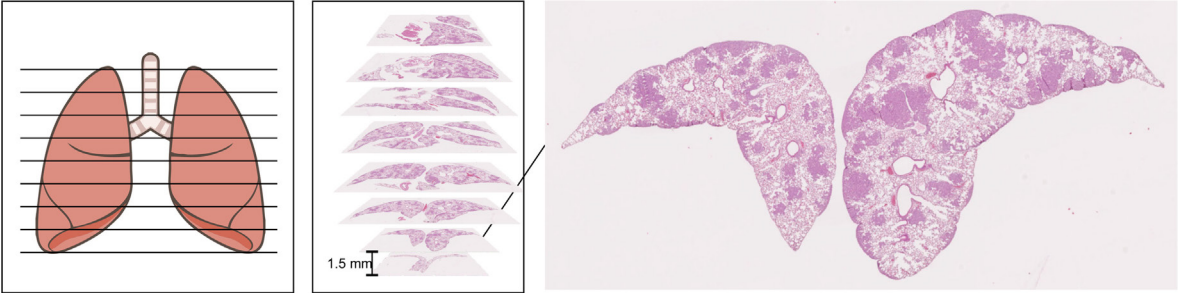


Figure S4. (a). Histology of lungs from mice injected with control and DOCK5 depleted MDA-MB-231 cells and sacrificed on day 28. Montages of systematically sampled lung sections from mice injected with control or DOCK5-depleted MDA-MB-231 cells. Lungs from mice injected with control MDA-MB-231 cells are enlarged and compacted with tumor cells and very little normal lung architecture remains (control). In contrast, mice injected with a pooled population of DOCK5-depleted MDA-MB-231 cells exhibit numerous distinct and partially coalesced tumor nodules interspersed among normal lung tissue (pool). Lungs from mice injected with DOCK5-kd cells (clone A) display few distinct tumor nodules and overall normal lung architecture. Lungs from mice injected with DOCK5-kd cells (clone B) are almost normal save for a few distinct tumor nodules. **(b)** Quantification of tumor burden in lungs from mice injected with control and DOCK5 depleted MDA-MB-231 cells and sacrificed on day 21. Total lung volume (reference space) and tumor volume was determined by stereological procedures as described in Methods. Embedded lungs were sectioned into 1.5 mm thick slabs in the indicated orientation (left panel). Next, the individual slabs were numbered and placed side by side with the anterior interface facing down on the flat surface in embedding chambers. This procedure allowed for re-embedding and subsequent sectioning of slabs (middle panel). Sections from each lung could be fitted on 2 microscope glass slides and processed for H&E staining. The stained samples were then imaged using an automated whole slide scanner and finally analyzed by newCAST software from Visiopharm. Sampling was done on each individual tissue slab section with a grid density and sampling coverage (50% of total area) adapted to allow typically 100-400 tumor positive spots in each cross section.

Figure S5. DOCK5 protein levels in tumor samples and adjacent histologically normal tissue from patients with mammary carcinoma. A SomaPlex reverse phase human breast cancer protein microarray slide (cat. no. PMA2-001-L) was probed with first DOCK5 antibody and next secondary antibody followed by development using TMB. The slide was scanned and the intensity of individual protein dots determined using Image J. **(a)** Select results in triplicate are show as follows: (1) BSA, negative control; (2) Raji cells with no signal, which is consistent with no detectable DOCK5 expression in lymphoma (Unigene Database, NCBI); (3) HeLa cells; (4) & (5) tumor 2 with lower DOCK5 levels in the tumor than in matched adjacent normal tissue; (6) & (7) tumor 11 with equal DOCK5 levels in tumor and matched adjacent normal tissue; (8) & (9) tumor 23 with higher DOCK5 levels in the tumor relative to matched adjacent normal tissue. **(b)** Ratio of DOCK5 expression between tumor sample and matched adjacent normal tissue. Triplicate dots for each individual tumor and control tissue sample were averaged and the ratio in intensity between tumor sample and matched adjacent normal tissue was determined. DOCK5 appears to be widely expressed in breast tumors, while significantly altered expression does not appear to correlate with any breast tumor subtype tested. Our results are consistent with mRNA expression profiles that indicate that DOCK5 is broadly expressed in a variety of epithelial tissues, including normal mammary gland and breast tumor tissue (Unigene Database, NCBI). **(c)** Grade, stage and TNM classification for individual tumor samples.

Table S1**Pathology of mice injected with MDA-MB-231 cells w/wo knockdown of DOCK5 expression.**

Group	Animal	Lungs	Mesenteric lymph nodes	Thorax	Heart	Other	Day of Sacrifice	Reason for Sacrifice
Control	1	Enlarged and spongy. Dark areas (L)	Slightly swollen	Bloody fluid			28	Hyperventilation
Control	2	Enlarged and spongy. Dark areas (L)					28	Hyperventilation
Control	3	Large. Dark spots	Small	Bloody fluid	Enlarged		28	Hyperventilation
Control	4	Large lungs, right lung black		Bloody fluid, blood clots	White spots	Liver: Pale Kidneys: Pale	28	Hyperventilation
Control	5	Many small spots, spongy	Slightly swollen	Bloody fluid			28	Hyperventilation
Control	6	Many small spots, spongy	Slightly swollen	Bloody fluid			28	Hyperventilation
Control	7	Enlarged. Dark spot (R)	Slightly swollen	Bloody fluid			28	Hyperventilation
Control	8	Enlarged. 1 big nodule, dark spot (L)	Slightly swollen				28	Hyperventilation
Control	9	Many spots	Slightly swollen				28	Hyperventilation
Control	10	Firm structure. 2 spots (R)	Slightly swollen	Bloody fluid			28	Hyperventilation
Control	11	Enlarged. Clear spots	Slightly swollen	Fluid	White spots		28	Hyperventilation
Control	12	Enlarged. Dark spots		Bloody fluid			28	Convulsion
Pool	13	Normal size. Surface uneven					28	Protocol
Pool	14	Enlarged. Surface uneven	Slightly swollen				28	Protocol
Pool	18	Surface uneven					28	Protocol
Pool	16	Enlarged, spongy and bloody. Nodules.	Enlarged			Uterus: Swollen, clear fluid	37	Hyperventilation
Pool	15	White spots, surface uneven					39	Hyperventilation
Pool	21	White spots, surface uneven. Fragile tissue				Intestines: Blood in appendix	39	Hyperventilation

Pool	20	Enlarged and spongy					44	Hyperventilation
Pool	22	Enlarged and spongy					46	Hyperventilation
Pool	17	Enlarged and spongy. White spots					47	Hyperventilation
Pool	19	White spots, surface uneven					52	Hyperventilation
Clone A	26	Normal					28	Protocol
Clone A	25	Enlarged and spongy. White spots, surface uneven					48	Hyperventilation
Clone A	30	Enlarged and spongy. White spots and uneven surface					49	Hyperventilation
Clone A	24	Enlarged and spongy. White spots, surface uneven					50	Hyperventilation
Clone A	23	White spots		Fluid			52	Hyperventilation
Clone A	28	Enlarged and spongy. White spots and uneven surface					54	Hyperventilation
Clone A	29	Enlarged and spongy. White spots and uneven surface			White spots		55	Hyperventilation
Clone A	27	Enlarged and spongy. Surface uneven. Hemorrhage					56	General
Clone B	38	Small	White, swollen			Liver: Enlarged, adhered to the diaphragm Spleen: Large, pale Intestines: Yellowish fatty tissues around the colon	26	Tumor and ruffled fur
Clone B	33	Normal					28	Protocol

Clone B	34	Enlarged and spongy. Surface uneven. Hemorrhage					52	Hyperventilation
Clone B	32	Enlarged and spongy. Surface uneven. Hemorrhage					58	Gait
Clone B	35	Enlarged. White spots, surface uneven		Fluid			63	Hyperventilation
Clone B	31	Enlarged. White spots granulated, hemorrhage at the top		A light spot on diaphragm in thorax		Legs: Swollen right hind leg Intestines: Yellowish	64	Paralysis in legs
Clone B	37	Enlarged. White spots. Surface uneven			Pale	Kidneys: Pale	70	Hyperventilation
Clone B	36						78	Paralysis in legs